



Simulated Responses of a Two-story Concrete Wall Building Shake-table Test

Anqi Gu^{1*}, Geoffrey W. Rodgers², Richard S. Henry³, Yiqiu Lu⁴ and Ying Zhou⁵

¹Post Doctoral Fellow, Department of Mechanical Engineering, University of Canterbury, Christchurch, New Zealand

²Professor, Department of Mechanical Engineering, University of Canterbury, Christchurch, New Zealand

³Associate Professor, Department of Civil and Environmental Engineering, University of Auckland, Auckland, New Zealand

⁴Professor, College of Civil Engineering, Tongji University, Shanghai, China

⁵Professor, College of Civil Engineering, Tongji University, Shanghai, China

*anqi.gu@canterbury.ac.nz (Corresponding Author)

ABSTRACT

A system-level shake-table test of a 2-story concrete wall building implementing state-of-the-art design concepts was conducted using the multi-functional shake-table array at Tongji University, as part of an international collaborative project. The test building was designed with a perimeter frame and exterior unbonded post-tensioned (UPT) walls in both directions. Different floor systems and wall-to-floor connections were incorporated in the test building to compare a number of design concepts and construction details. A range of energy dissipation devices were installed at the wall bases and/or slotted-beam joints of the test building. The test results of the shake-table testing not only verified the desirable seismic performance of the UPT wall buildings, but also provided a shaking-table dataset for the UPT wall modelling verification.

The objective of this study is to assess the accuracy of current modelling methods and identify the gaps between the simulation and test results. Planar frame models adopting current modelling methods were selected to represent the test building in the longitudinal and transverse directions, respectively. In the models, fiber hinge elements were used to simulate the UPT wall bases and a modified multi-spring method was adopted to simulate the slotted-beam joints with and without energy dissipaters. Nonlinear time-history analyses of the models were conducted considering design-based earthquake (DBE) and maximum considered earthquake (MCE) intensities. The simulation results showed that the planar frame models established in this study could reasonably capture both the global and local responses of the test building under different design configurations. However, the models underestimated the peak base moment of the test building by an average of 36% and 26% in the longitudinal and transverse direction, respectively. The underestimated lateral strength was attributed to the contribution of wall-to-floor interaction in the test building and is the focus of further research.

Keywords: Unbonded post-tensioned wall, precast concrete, shake-table test, finite element model, analysis and computation.

INTRODUCTION

A system-level shake-table test of a full-scale two-story concrete wall building was conducted in 2019. The test building consisted of UPT walls and perimeter frames. The UPT walls were designed to provide lateral resistance in all the design configurations. The perimeter frames were designed as gravity frames, while contributing some moment resistance when energy dissipating (ED) devices were installed at the beam-to-column joints. The beam-to-column joints in the test building are designed using a slotted-beam joint concept to reduce the axial elongation that can create frame dilation. The column bases are also connected to the foundation as pins. The connection detailing between the floor slab system and the perimeter frames were constructed to reduce the wall-to-floor interaction effect. In addition, various combinations of the ED devices were considered in the test building. The test results of the shake-table testing verified the desirable seismic performance of the UPT wall buildings [1]. This test building also provided a dataset for the UPT wall modelling verification.

The objective of this study is to assess the accuracy of current modelling methods and identify the gaps between the simulation and test results. The planar frame models were established in *OpenSees* using fiber hinge model for the UPT wall and modified multi-spring model for the slotted-beam joints. The fiber hinge model was used to model the UPT walls and validated with the cyclic loading tests and shake-table test results [2-3]. The multi-spring model was adopted to predict the response of the slotted-

beam joint in the cyclic loading tests [4]. A modified multi-spring model for the slotted-beam joints was proposed for the planar frame model. The modified multi-spring model was identical with the multi-spring model except that the top hinge regions of the slotted-beam joints were modelled using fiber beam-column elements representing the concrete region and twoNodeLink elements representing the longitudinal and diagonal hanger reinforcements. To verify the adopted modelling method, the material properties of the planar frame models were calibrated by the measured materials properties, the material models and parameters chosen for the ED devices were verified with the cyclic test results of the corresponding samples, and then simulation results were compared with the test results for different design configurations, ground motion types and intensities. Additional description of the modelling methods could be found in Gu et al. [5].

PLANAR FRAME MODELS ESTABLISHMENT

This section briefly introduces the establishment of the planar frame models which represent the Grid A and Grid 1 perimeter frames in the test building. Figure 1(a) illustrates the overall dimensions of the test building. The test building plan dimensions were 5.4×8.95 m, and the total height of the building from the foundation surface was 8 m, with each story 4 m high. The test building had a double-tee precast floor system on level 1 (L1) running longitudinally and a composite floor system at level 2 (L2) running transversely, as presented in Figures 1(b) and (c). In the longitudinal direction, a flexible wall-to-floor link slab connection was applied in the L1 floor slab, and the wall was connected to the composite floor directly in L2. In the transverse direction, the uplift of the UPT walls was isolated from the perimeter frames by the isolated Wall-to-Floor connection. The design information of the test building and the test dataset are available on DesignSafe-CI [6], and a summary of the test results has been published by Henry et al. [1].

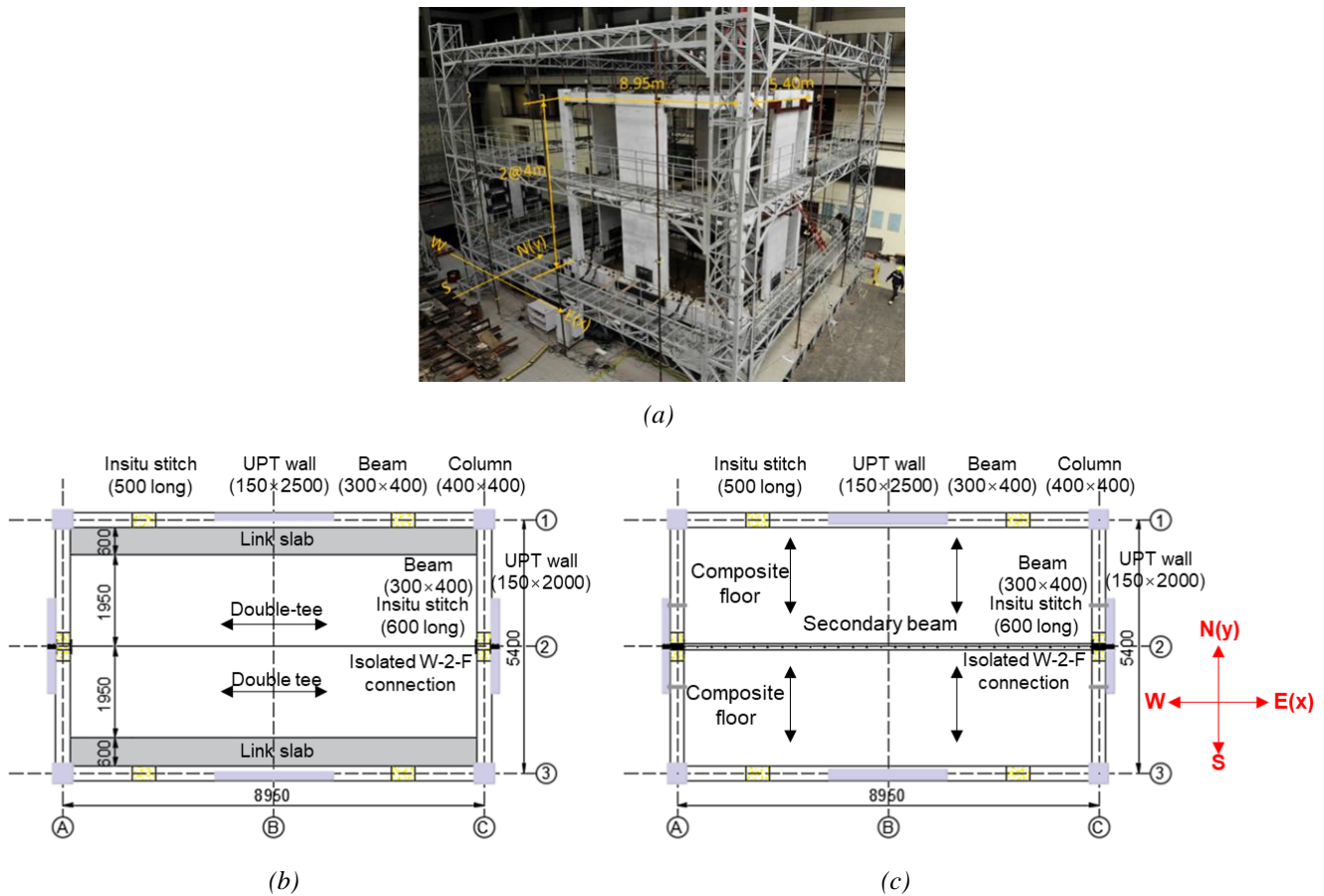


Figure 1. Details of the test building: (a) on-site photo, (b) L1 layout, (c) L2 layout.

Material properties

Concrete cylinder tests were conducted before the shake-table testing. The confined concrete properties at the UPT wall bases were calculated based on the constitutive model proposed by Mander [7]. The concrete test results of the Wall A and Wall 1 were adopted for the planar frame models. Figures 2(a) and (b) show the concrete compressive stress-strain curves used in the planar frame models. The confined concrete and unconfined concrete materials were modelled using the Concrete02 uniaxial material. The stirrups in the confined concrete regions were HPB 8 (plain bar, diameter 8 mm, $f_y = 332$ MPa, $f_u = 456$ MPa)

and the average ultimate strain of the stirrups was 0.117. The concrete compressive strengths of the beam components at L1 and L2 were 58.4 MPa and 56.1 MPa, respectively. The concrete compressive strengths of the column components at L1 and L2 were 58.6 MPa and 57.2 MPa, respectively. The PT bars were modelled using the Steel02 uniaxial material with bilinear stress-strain curves, as shown in Figure 2(c). For the 25 mm PT bars (1080PSB), the ultimate strain was 0.047 and the elastic modulus was 202 GPa. For the 32 mm PT bars (1080PSB), the elastic modulus was 198 GPa. Table 1 listed the material properties to model the slotted-beam joints.

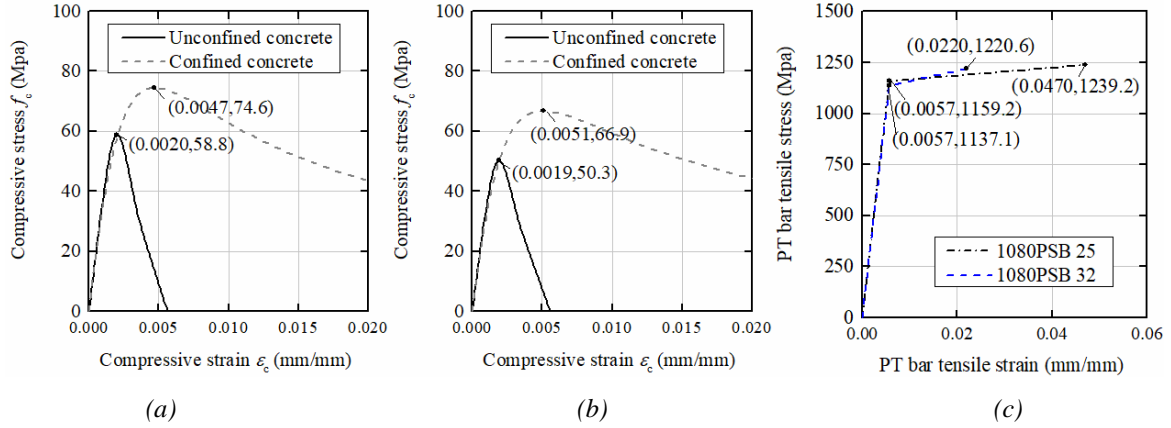


Figure 2. Material properties of the UPT walls: (a) concrete stress-strain curves of Wall 1, (b) concrete stress-strain curves of Wall A, (c) PT bars stress-strain curves.

Table 1. Material Properties for Slotted-beam Joints Modelling.

Types	Location	f_y / f_c (MPa)
HD16	Beam shear hanger	529.8
HD20	Beam shear hanger	506.7
	Beam longitudinal reinforcement	507.7
Concrete	Top hinge for L1	36.2
	Top hinge for L2	36.6

Energy dissipating devices

A total of three types of ED devices, which were grooved steel fuses [8], high force-to-volume energy dissipation (HF2V) [9-10] and nonlinear viscous dampers [11], were incorporated in the test building considering in three different design configurations. The combination of the ED devices in different design configurations are presented in Table 2. The D1 configuration represented the design target drift of 1%, while the D2 configuration represented the design target drift of 2%. The performances of ED devices were important to the simulation accuracy of the planar frame models. The mechanical properties of the steel fuses used in D1a were modelled using the ReinforcingSteel uniaxial material, while the properties of the fuses used in D2 were modelled using the Steel02 uniaxial material. The fuses material parameters were calibrated using the cyclic testing results for the sample fuses. HF2V devices used in D1b and D1c were modelled using a Steel01 material because they were relatively insensitive to velocity, with a velocity component of approximately 0.12 [9-10]. The viscous dampers used in D1b were modelled using the ViscousDamper material, and the material stiffness parameters were calculated as 131 kN/mm and 1380 kN/mm according to Akcelyan et al. [12]. The parameters chosen for the ED devices were verified with the cyclic test results of the corresponding ED samples.

Table 2. ED Devices for Each Design Configuration.

Design building configuration	Slotted-beam	Wall bases
D1	D1a	steel fuses
	D1c	HF2V
	D1b	HF2V
D2	-	viscous dampers
		steel fuses

Finite element models

Planar frame models adopting current modelling methods were selected to simulate the test building dynamic response in both directions. Schematic representations of planar frame models in both the longitudinal and transverse directions for the D1a configuration established in *OpenSees* are shown in Figure 3. An accurate simulation of the UPT wall base behavior and the slotted-beam joints was important for modelling the test building response. The UPT wall bases were simulated using a fiber

beam-column element, and elastic beam-column elements were used to model the wall panels that suffered no damage during testing. The fiber hinge length was set to be $1.6 t_w$ for the model developed which is within the range of recommended values by prior researchers [2, 13-14] and approximately equal to the neutral axis depth observed at the wall base during the tests, and t_w represents the wall thickness. The cross section of wall bases and the PT bar details could be found in Figure 4. The beams and columns in the perimeter frames were modelled using elastic Beam-Column elements, and the column bases were pinned. Since the beam and column components in the test building suffered little damage, the section moment of inertia for both the beam and column elements were set to be $0.6 I_{gross}$ [15], and I_{gross} represents the moment inertia of the gross section. Truss elements were chosen to represent the PT bars and steel fuses. The transverse direction model was similar to that in the longitudinal direction, except for the fact that the UPT wall in the transverse direction was offset from the frame. The isolating wall-to-floor connections were also considered in the transverse direction frame model using zeroLength elements to release the vertical constraints between the UPT wall and the adjacent beams.

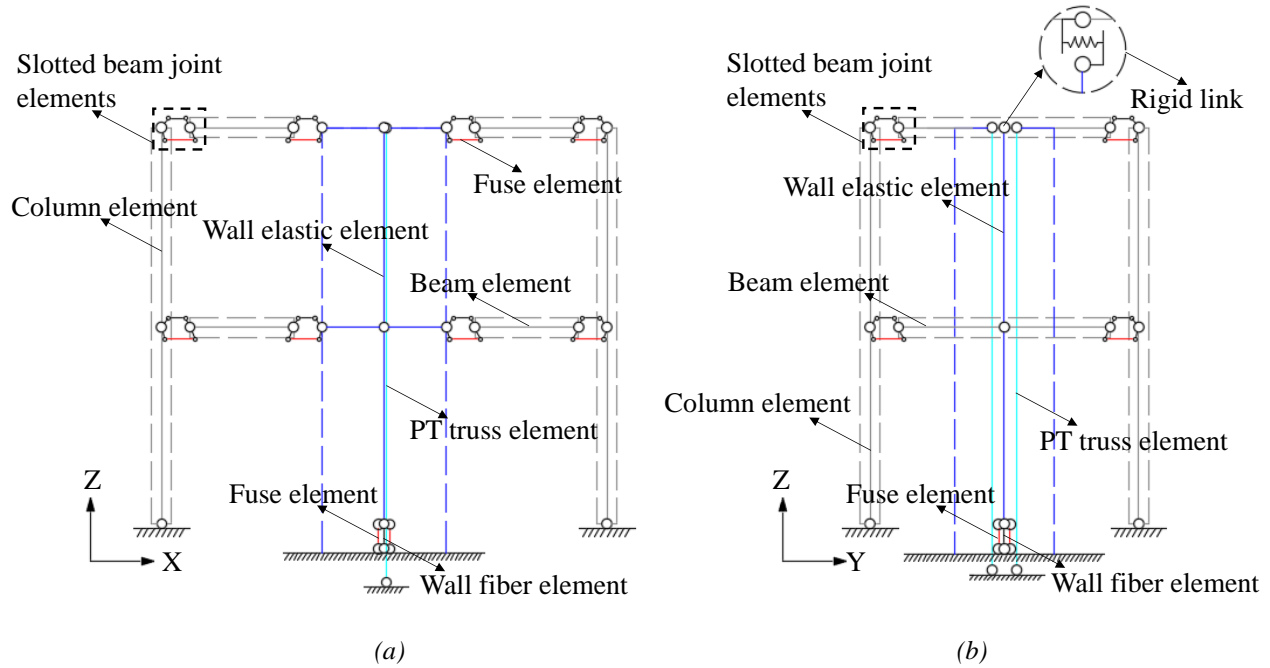


Figure 3. Schematic representations of models for D1a configuration: (a) longitudinal direction frame, (b) transverse direction frame.

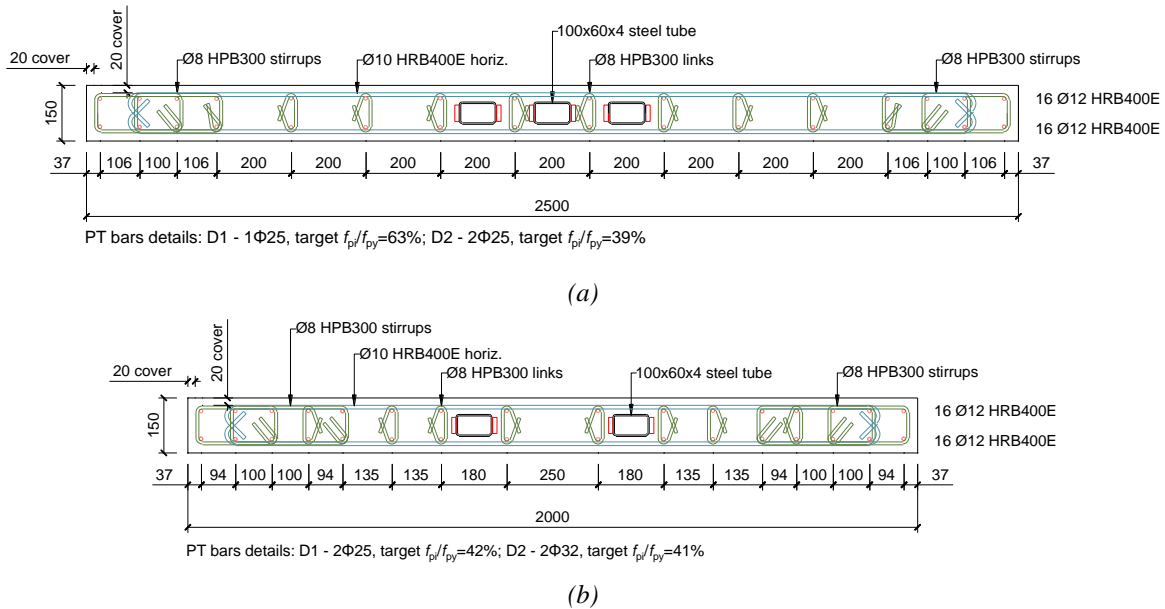


Figure 4. Cross sections of wall bases: (a) Wall I base, (b) Wall A base.

The total seismic weight of the test building, including the self-weight and additional mass, equaled 522 kN and 357 kN for L1 and L2, respectively. The planar models represented half of the building lateral-resistance, so half of the total seismic mass was accumulated at the wall node at each level. The gravity loads were applied as point loads to the walls and column nodes in the model. For the corner columns and UPT walls in the longitudinal direction, the gravity loads were calculated according to the tributary areas. Rayleigh damping was used to model the inherent damping, with damping ratios of 2% for T_1 and T_{eff} for the design-level earthquake (DBE) and maximum considered earthquake (MCE) intensities, where T_1 represents the fundamental period of the planar frame model, and T_{eff} represents the effective period at the design target drift. Additional description of the establishment of the planar frame models could be found in Gu et al. [5].

ANALYSIS RESULTS FROM THE PLANAR FRAME MODELS

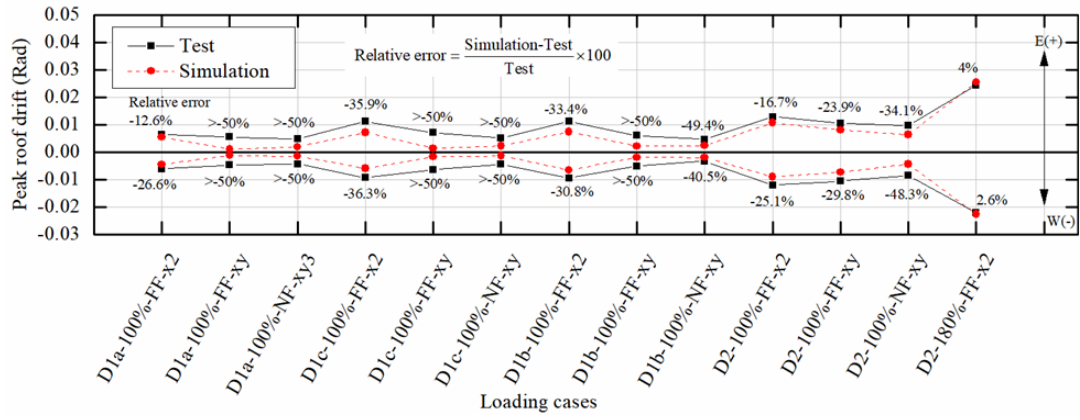
In this section, the nonlinear time-history analysis results of the planar frame models were compared with the test results. The input records of the loading cases under DBE and MCE intensities were considered for the time-history analysis. The input records include the Far-Field (FF) and Near-Field (NF) records. The FF record was the 1995 Kobe earthquake Nishi-Akashi station record, which was used in the unidirectional (tagged as x or y) and bi-directional (tagged as xy) loading cases. The NF record was the 1989 Loma Prieta earthquake Saratoga-Aloha Ave station record, which was used in the bi-directional loading cases. In the bi-directional loading cases, the primary component of the earthquake record was input in the transverse direction of the test building, and the secondary component of the earthquake record was input in the longitudinal direction. For the considered loading cases under the MCE intensity, the DBE FF records with a higher scale factor were used in unidirectional loading cases. The simulated and experimental global responses were compared under the DBE and MCE intensities. The local responses are presented for unidirectional earthquake input loading cases under the MCE intensity.

Global responses of the time-history analysis

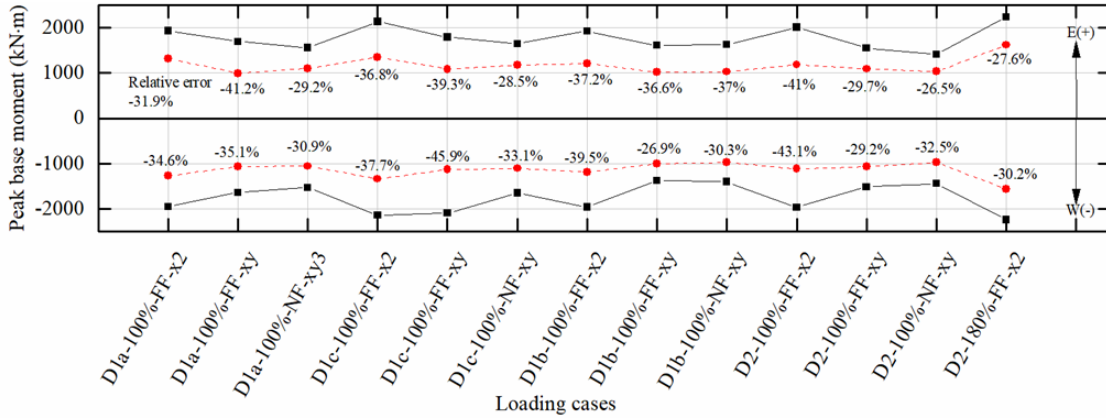
Figures 5 and 6 summarize the peak roof drifts and base moments in both the positive and negative loading directions, comparing both the simulation responses and experimental results. The following key observations were made from the global model results:

- 1) The model tended to underestimate peak drifts in the longitudinal direction for the DBE loading cases. The analytical results for the longitudinal frame in the NF bi-directional loading cases were closer to the test results compared with the analytical results in the FF bi-directional loading cases, except for the D2 bi-directional loading cases. For the MCE intensity, the model closely predicted the peak drifts in the longitudinal direction.
- 2) In the transverse direction, the model peak roof drifts were smaller than the measured drifts from the test building during the DBE loading cases, while the model overestimated the peak drifts during the MCE loading cases.
- 3) A comparison of the model and test peak roof drifts showed that the relative errors of peak drifts in the transverse direction were on average larger than that in the longitudinal direction for the MCE loading cases, while smaller than that in the longitudinal direction for the DBE loading cases.
- 4) The models in both the longitudinal and transverse directions underestimated the peak base moment considering all the loading cases. In particular, the planar frame models without considering the wall-to-floor interaction effect would predict the peak base moment on average 36% and 26% smaller than the test results in the longitudinal and transverse direction, respectively.

The comparison presented in Figures 5 and 6 indicates that the planar frame models generally captured the global responses of the test building better for the unidirectional tests than the bi-directional tests, which is perhaps not surprising given 2D planar models were used rather than a full 3D model. Although a full 3D model could be better used for investigating the components' interaction and coupling of the two orthogonal 2D models, development of the full 3D model is beyond the scope of this study. And ongoing work is focused on the 3D model. In addition, despite the connection detailing adopted the wall-to-floor interaction effects were still significant and contributed to the planar frame model underestimation of the peak base moments for all the loading cases. This observation is supported by a prior comparison of the overstrength of the test building to the design values [1].



(a)



(b)

Figure 5. Comparison of simulation and test peak global responses for loading cases in the longitudinal direction: (a) roof drift, (b) base moment.

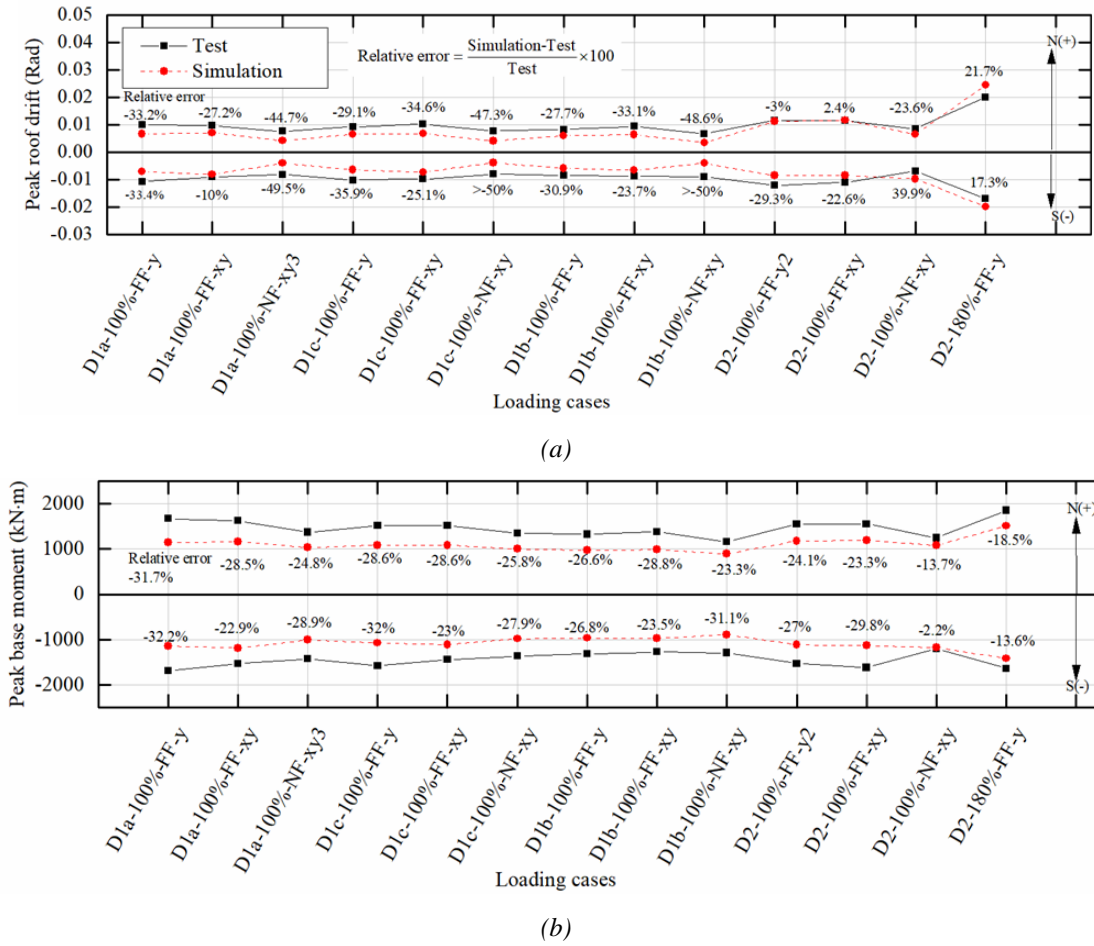


Figure 6. Comparison of simulation and test peak global responses for loading cases in the transverse direction: (a) roof drift, (b) base moment.

A comparison of the D1a planar frame model and test global responses for the DBE unidirectional tests are shown in Figure 7. In the longitudinal direction, the time-history analytical results generally matched the test results, except that the model results underestimated the test building peak response. In the transverse direction, the analytical results for the time-history matched with the test results over the first 10s, while the model response damped out faster than the test results in the later part of the test. The potential reason for the faster decay observed in the simulation results (which is also seen in other design configurations) is that the ED devices' nuts were observed to loosen slightly during testing, creating a small amount of free-travel on load reversals that reduced the efficiency of these devices and was not considered in the models.

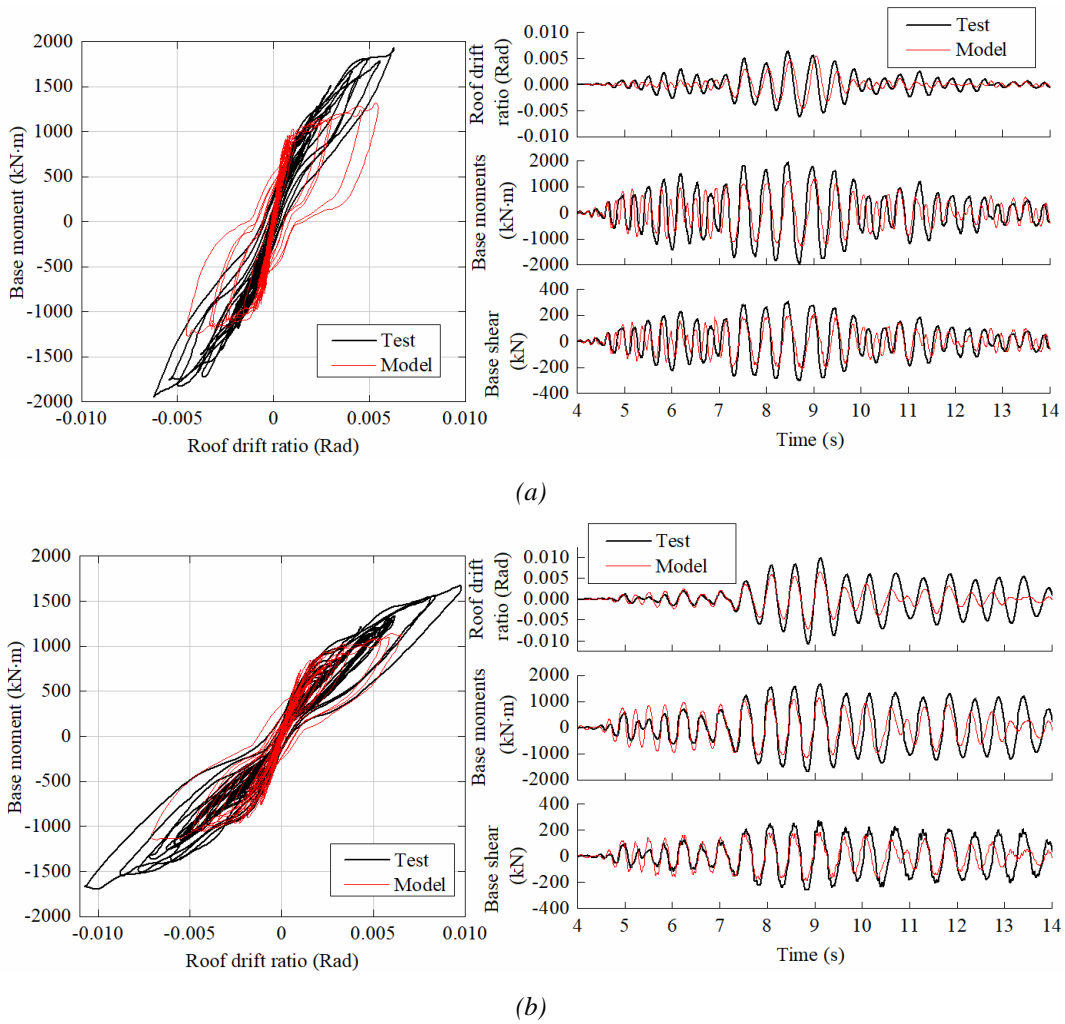


Figure 7. Comparison of simulation and test results for D1a DBE unidirectional shaking: (a) longitudinal direction, (b) transverse direction.

A comparison of the D2 model analytical and test global responses for the MCE unidirectional tests are shown in Figure 8. The simulated peak roof drifts were comparable to that of the test building in both directions, but the peak base moments and shears calculated by the models were still smaller than the test results. This finding is consistent with the simulation response at the DBE intensity. Phase differences were found between the simulation and test time-history responses after 10s in longitudinal direction and 23s in transverse direction. The wall-to-floor interaction effect was considered to be the main cause of the phase differences between the simulation and test results with the additional strength and stiffness influencing the secant period of vibration during periods of uplift and will contribute to some phasing effects between the simulation and test results.

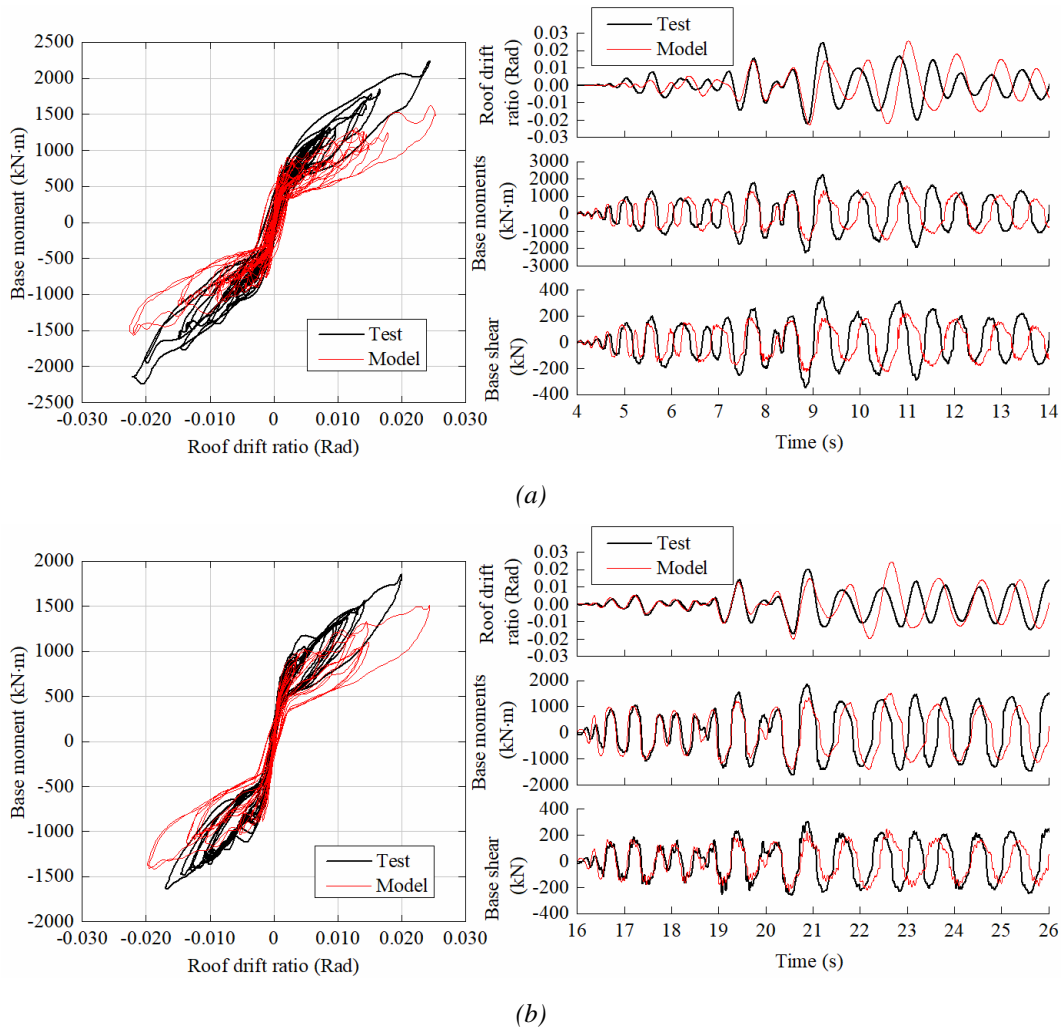


Figure 8. Comparison of simulation and test results for D2 MCE unidirectional shaking: (a) longitudinal direction, (b) transverse direction.

Local response of the time-history analysis

The local responses of the UPT wall obtained from the model in the longitudinal direction considering the D2 configuration were compared with the test results under the MCE intensity, and are presented in Figure 9. The predicted neutral axis depths at the peak drifts and the broad trends in the response generally matched the test results. The wall uplifts and PT bar force closely matched the test results. The results presented in Figure 9 proved that the analytical models adequately captured the local responses of the UPT walls as they uplift and rock.

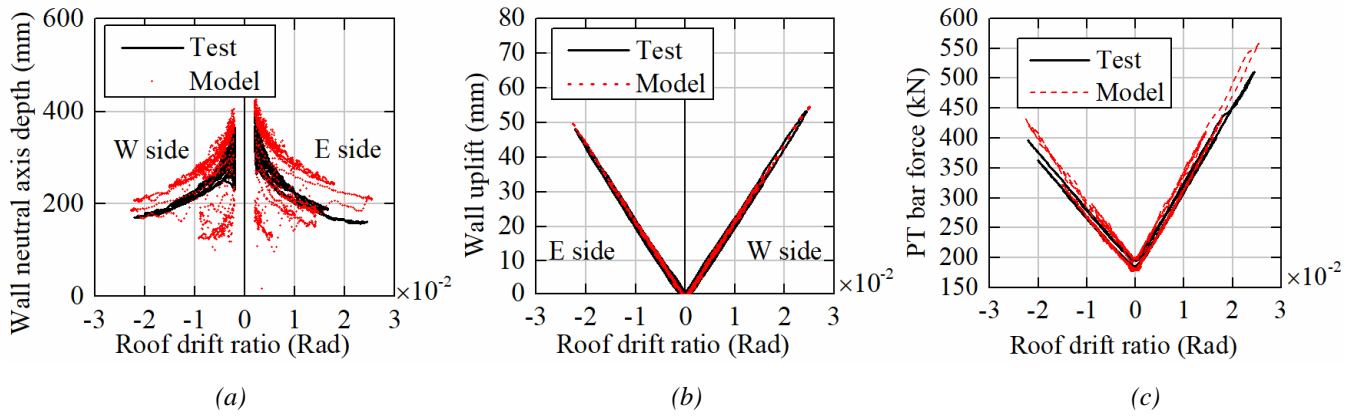


Figure 9. Comparison of Wall 1 responses for D2 MCE unidirectional shaking: (a) neutral axis depth, (b) wall uplift, (c) PT bar force at wall W side.

Comparisons of simulation and test results about the slotted-beam rotation in the MCE unidirectional tests are presented in Figure 10. In both directions, the analytical model underestimated the neutral axis depth during slot opening and slightly overestimated the neutral axis depth during slot closing. However, the simulated neutral axis depth cyclic response generally followed similar trends to that response of the test results. The comparisons showed that the slotted-beam joints modelling method was suitable to capture the building response.

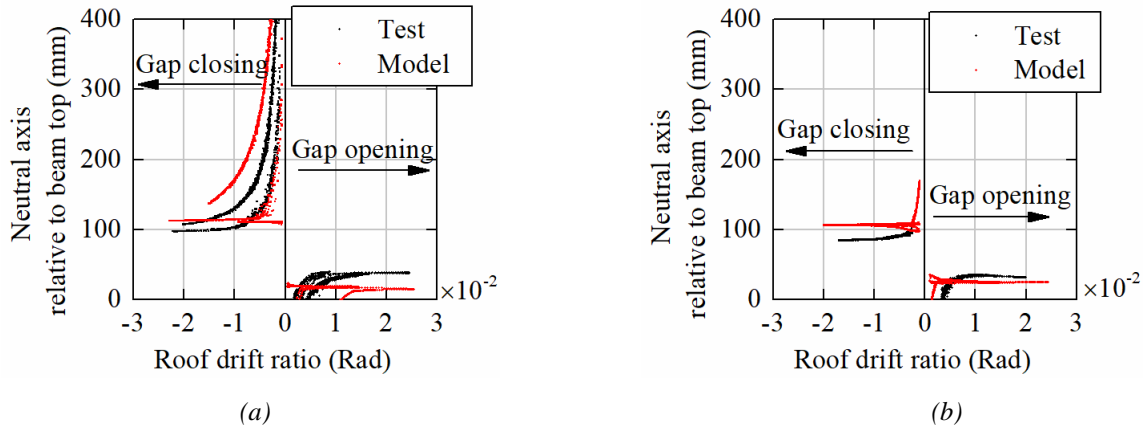


Figure 10. Comparison of neutral axis depths of slotted-beam joints for D2 MCE: (a) L2 slotted-beam 1@A in longitudinal unidirectional shaking, (b) L1 slotted-beam A@3 in transverse unidirectional shaking.

CONCLUSIONS

Planar frame models representing the perimeter frame in both directions were established for a previously tested 2-story low-damage concrete wall building. Nonlinear time-history analysis was performed for the planar frame models. The simulation results showed that the planar frame models established in this study could reasonably capture both the global and local responses of the test building under different design configurations. The following conclusions were drawn from a comparison of the key simulation and test results for the global and local responses:

1. The peak roof drift response results from the models with the different design configurations provided reasonable estimates compared with the test roof drift responses in the unidirectional tests for DBE and MCE intensities. In both the longitudinal and transverse models, the calculated peak roof drifts were smaller than the responses measured during the tests for the DBE intensity and slightly larger than the test results for the MCE intensity. This difference was potentially attributed to the wall-to-floor interaction effect which was not included in the planar models.
2. The simulated peak base moment responses were also smaller than the responses measured from the tests in both directions. It is also notable that the planar frame models without considering the wall-to-floor interaction effect would calculate the peak base moment on average 36% and 26% smaller than the test results in the longitudinal and transverse direction, respectively.
3. Discrepancies between the model and test global responses under bi-directional tests indicated that the planar models failed to consider the bidirectional loading effects on the test building's responses. In addition, the longitudinal frame was more

influenced by the bi-directional loading effects. The reason could be that the secondary component of seismic record was input in the longitudinal direction.

4. The local responses of the UPT wall and the slotted-beam joints were adequately captured by the model when comparing to the test results. The local response comparisons confirmed that the fiber hinge modelling and modified multi-spring modelling techniques used were appropriate to capture the response of such systems.

ACKNOWLEDGMENTS

The authors would like to acknowledge the financial support provided by International Joint Research Laboratory of Earthquake Engineering (Grant No. ILEE-IJRP-P2-P4-2017), and the New Zealand Ministry of Business, Innovation and Employment (MBIE) Building System Performance. The authors also acknowledge financial support provided by the National Key Research and Development Program (Grant No. 2016YFC0701101). This project was also partially supported by QuakeCoRE, a New Zealand Tertiary Education Commission-funded Centre, and a Royal Society Te Apārangi Rutherford Discovery Fellowship.

REFERENCES

- [1] Henry, R.S., Zhou, Y., Lu, Y., Rodgers, G.W., Gu, A., Elwood, K.J. and Yang, T.Y. (2021). "Shake-table test of a 2-storey low-damage concrete wall building". *Earthquake Engineering & Structural Dynamics*, 51(12), 3160-3183.
- [2] Watkins, J., Henry, R. and Sirtharan, S. (2013). "Computational modelling of self-centering precast concrete walls." In *4th ECCOMAS Thematic Conference on Computational Methods in Structural Dynamics and Earthquake Engineering*, Kos Island, Greece.
- [3] Watkins, J., Sirtharan, S., Nagae, T. and Henry, R.S. (2017). "Computational modelling of a four storey post-tensioned concrete building subjected to shake table testing". *Bulletin of the New Zealand Society for Earthquake Engineering*, 50(4), 595-607.
- [4] Au, E. (2010). *The Mechanics and Design of a Non-tearing Floor Connection Using Slotted Reinforced Concrete Beams*. Department of Civil and Natural Resources Engineering, University of Canterbury, Christchurch, New Zealand.
- [5] Gu, A., Zhou, Y., Henry, R.S., Lu, Y. and Rodgers, G.W. (2022). "Simulation of shake-table test for a two-story low-damage concrete wall building". *Structural Control and Health Monitoring*, 29(10).
- [6] Henry, R.S., Lu, Y., Zhou, Y., Rodgers, G.W., Gu, A., Yang, Q., Elwood, K.J. and Yang, T.Y. (2020). "Dataset on shake table test of a low-damage concrete wall building". DesignSafe-CI. DOI: [10.17603/ds2-ncac-sg36](https://doi.org/10.17603/ds2-ncac-sg36)
- [7] Mander, J.B., Priestley, M.J.N. and Park, R. (1998). "Theoretical stress-strain model for confined concrete". *Journal of Structural Engineering*, 114(8), 1804-1826.
- [8] Liu, R., McHaffie, B. and Palermo, A. (2018). "Improving post-tensioned rocking bridge columns for large and multiple earthquake events." In *17th US-Japan-New Zealand Workshop on the Improvement of Structural Engineering and Resilience*, Queenstown, New Zealand.
- [9] Rodgers, G.W., Solberg, K.M., Chase, J.G., Mander, J.B., Bradley, B., Dhakal, R. and Li, L. (2008). "Performance of a damage-protected beam-column subassembly utilizing external HF2V energy dissipation devices". *Earthquake Engineering & Structural Dynamics*, 37(13), 1549-1564.
- [10] Rodgers, G.W., Mander, J.B., Chase, J.G., Leach, N.C. and Denmead, C.S. (2008). "Spectral analysis and design approach for high force-to-volume extrusion damper-based structural energy dissipation". *Earthquake Engineering & Structural Dynamics*, 37(2), 207-223.
- [11] Golzar, F.G., Rodgers, G.W. and Chase, J.G. (2018). "Design and experimental validation of a re-centring viscous dissipater". *Structures*, 13, 193-200.
- [12] Akcelyan, S., Lignos, D.G. and Hikino, T. (2018). "Adaptive numerical method algorithms for nonlinear viscous and bilinear oil damper models subjected to dynamic loading". *Soil Dynamics and Earthquake Engineering*, 113, 488-502.
- [13] Perez, F.J., Sause, R. and Stephen, P. (2007). "Analytical and experimental lateral load behavior of unbonded posttensioned precast concrete walls". *Journal of Structural Engineering*, 133(11), 1531-1540.
- [14] Gavridou, S., Wallace, J.W., Nagae, T., Matsumori, T., Tahara, K. and Fukuyama, K. (2017). "Shake-table test of a full-scale 4-story precast concrete building. II: Analytical studies". *Journal of Structural Engineering*, 143(6), 04017035.
- [15] Twigden, K.M. and Henry, R.S. (2019). "Shake table testing of unbonded post-tensioned concrete walls with and without additional energy dissipation". *Soil Dynamics and Earthquake Engineering*, 119, 375-389.